THE FILTRATION MECHANISM AND MICRO-OBSERVATION OF SOIL-GEOTEXTILE SYSTEMS UNDER CYCLIC FLOWS

Rong-Her Chen[1], Chia-Chun Ho[2] and Wen-Bin Chung[3]

ABSTRACT

Geotextile filters have been used frequently in revetments for protection of riverbanks, levees, seashores, *etc*. The filters may be subjected to different flow conditions such as unidirectional or cyclic flows. Besides, the period of flow may vary from short to long due to the fluctuation of water table caused by sea waves, boats, tidal activity, or periodic drawdown of water for irrigation purposes. Due to few literatures on cyclic flow studies, this paper presents the investigation on soil-geotextile filtration mechanisms under long-term cyclic flows using a self-developed apparatus. The soil samples are composed mainly of sand, with 0-20% fines content of silts and clays. The factors taken into account are overburden pressure and cyclic flow periods ranging from long to short, in order to simulate a range of waves. A stereomicroscope is utilized to observe the microstructure of the geotextile filter after testing. The results show that both the overburden pressure and the fine soil content play important roles in the filtration, soil boiling, and settlement behaviors of a soil-geotextile filtration system. Furthermore, the microscopic images of the geotextile show that soil clogging under cyclic flows is not so serious as that under unidirectional flows. Besides, a bridging network can be formed under long-term cyclic flows in the areas near the filter that are not supported by marbles.

Key words: Geotextile, filter, cyclic flow, soil erosion, bridging network.

1. INTRODUCTION

Filtration is a process that suspended or dissolved solids are separated from a fluid as it flows through a porous media. A soil filter is used for this purpose. In the filter design, it is based on parameters such as channel morphology, concentration of suspended solids or dissolved solids characteristics, and fluid properties such as viscosity and density. Another important factor is the source of driving forces which may be hydrodynamic, gravity, suction or positive seepage pressures.

The water infiltrating through the pores of a soil-geotextile system may change the soil structure and decrease the intrinsic coefficient of hydraulic conductivity. To prevent this phenomenon, a suitable geotextile should be selected to impede sufficiently the movement of soil particles and to build a natural filter layer. In turn, this filter layer may restrain smaller particles migration until a stabilization state is established. In general, the faster a natural filter establishes the smaller amount of soil particles will migrate.

The use of geotextile filters for revetments to protect riverbanks, levees, seashores has become popular. The filters may be subjected to different flow conditions such as unidirectional or cyclic flows. Besides, the period of cyclic flows may vary from short to long due to the fluctuation of water table caused by sea waves, boats, tidal activity, or periodic drawdown of water for irrigation purposes. A stable soil-geotextile filter system must be formed under these circumstances.

Under cyclic flow condition, soil particles may migrate or be washed away that induces failure of a revetment. For example, a revetment failure has been reported by Chen *et al*. (2008). The revetment was composed of a layer of concrete cover lain on the top of a soil slope. The constituent of the soil was mainly sands with about 10% silt and clay. The filter was made of gravels wrapped by geotextiles and placed at the drainage holes. The revetment of 1.6 km long failed several months after it had been completed. According to the investigation, the cause was due to periodic drawdown of water about 2 m high per week. In addition to this case, there are many tidal lands and harbor structures built in western Taiwan. The tide causes variation in the groundwater level which may lead to soil loss or ground settlement and jeopardize structures. The rubble-mound groin is often used for protecting coastlines. In Taichung Port, the loss of soil at one location of the south levee damaged a road just behind the levee. This kind of damage also occurred in the Changbin Industrial Center where settlements, cracks, sinkholes were found on the surface of the road adjacent to the levee (Hsu, 2007; Liao and Chu, 2002).

The studies of the particle structure and the hydraulic characteristics in the zone adjacent to a filter are essential to understand the filtration mechanism under cyclic flows. However, most of previous researches considered simpler conditions, such as unidirectional flow, than real in-situ conditions (Giroud, 1982; Lawson, 1982; Chen and Chen, 1986; Luettich *et al.,* 1992; Aydilek, 2006). Very few recent laboratory studies on geotextile filters have examined conditions of dynamic, cyclic, and pulsating flows (Cazzuffi *et al.,* 1999; Fannin and Pishé, 2001; Chew *et al.,* 2003; Chen *et al.,* 2006). Due to few literatures of cyclic flow studies, this paper presents the investigation on soil-geotextile filtration mechanisms under long-term cyclic flows by employing a self-developed apparatus (Chen *et al.,* 2008). A stereomicroscope is also utilized to observe the inside condition of geotextile filters as well as the adjacent soil structures.

Manuscript received July 31, 2008; revised October 9, 2008; accepted October 9, 2008.

[1] Professor (corresponding author), Department of Civil Engineering, National Taiwan University, No. 1, Sec. 4, Roosevelt Rd., Taipei, 10617 Taiwan (e-mail: rongherchen@ntu.edu.tw).

[2] Postdoctoral fellow, Department of Civil Engineering, National Taiwan University, No. 1, Sec. 4, Roosevelt Rd., Taipei, 10617 Taiwan (e-mail: d90521023@ntu.edu.tw).

[3] Former master's student at National Taiwan University, No. 1, Sec. 4, Roosevelt Rd., Taipei, 10617 Taiwan (e-mail: bing830202@msn.com).

2. FILTRATION MECHANISMS

Regarding a natural filter formation, two mechanisms based on perpendicular flow conditions have been proposed by Rollin and Lombard (1988), *i.e.*, the bridging network and the vault network formations (Fig. 1). The bridging network formation usually occurs in non-cohesive soils. At first, large particles are stopped at the surface of a geotextile structure. In turn, these particles retain smaller particles; this process continues until the soil stabilizes. On the other hand, the vault network formation occurs in non-cohesive soils with appreciable clay content or in cohesive soils. Vaults are initiated by geotextile fibers, as shown in a photographic cross-section of a geotextile sample collected in-situ and presented schematically in Fig. 2.

Moreover, Scheidegger (1957) divided filtration into three classes: medium, cake, and depth filtrations. In the medium filtration, particles larger than the filter entry pores are retained, generally at surface openings or shortly inside the upstream face. This type of filter thus behaves like a sieve. In the depth filtration, the particles smaller than the filter pores and the dissolved materials are intercepted and retained within the filter section. In the cake filtration, solids do not enter the filter to a great extent, but accumulate on or in front of the surface of the filter. Soil filters are a variation of cake filtration to some extent.

The forming process of a filter cake in soil-geotextile systems is quite complicated. Mlynarek *et al.* (1991) summarized the occurrence mechanisms as the five phases presented in Fig. 3.

Nevertheless, a distinction must be made between unidirectional flow and cyclic flow in filtration design using geotextiles. Though it is believed that a natural bridging network is induced in the soil adjacent to the geotextile during unidirectional flow, this network may or may not develop for long-term cyclic flows. For instance, under impacting water flow such as wave activity (short-term cyclic flow less than 10 sec/cycle), the influence of changing direction of flow and associated seepage forces can destabilize such a network (Giroud, 1982; Köhler, 1993). This study specifically focused on long-term cyclic flows due to tidal activity or water drawdown such as for irrigation purposes described above.

3. APPARATUS FOR CYCLIC FLOW TEST

To study the filtration mechanism of geotextiles under cyclic flows, an apparatus was developed at National Taiwan University (Fig. 4), with some modifications of the cyclic flow model of ENEL, Italy (Cazzuffi *et al.*, 1999). This apparatus is capable of simulating cyclic flow normal to the soil-geotextile interface. It consists of a cyclic wave generator, an acrylic sample chamber, a water reservoir and wash-out collecting tank, and a vertical pressure application system. Figure 5 shows a detailed schematic view of the internal set-up of the chambers. The acrylic specimen cylinders consisting of upper and lower chambers are for the convenience to observe the state of soil erosion. The lower chamber contains marbles which simulate the secondary armor layer of a revetment. A porous steel plate is placed below the lower chamber to maintain the marbles. The geotextile specimen is laid on the marbles and clamped in the groove between upper and lower chambers; and then the soil specimen is filled in the upper chamber. There are four pore pressure transducers (P01, P02, P03 and P04) placed at different positions to monitor the fluctuation of pore pressure. The measured pore pressure can provide information regarding various phenomena such as blinding, clogging, or blocking. Ports P01 and P02, with a distance of only 30 mm, are located just above and below the level of geotextile specimen, respectively. The intention is to capture the interaction between geotextile and soil close to the interface (Palmeira and Fannin, 2002). In addition, two settlement gages, S01 and S02, are mounted on the top of the porous steel plate to obtain the average settlement during testing.

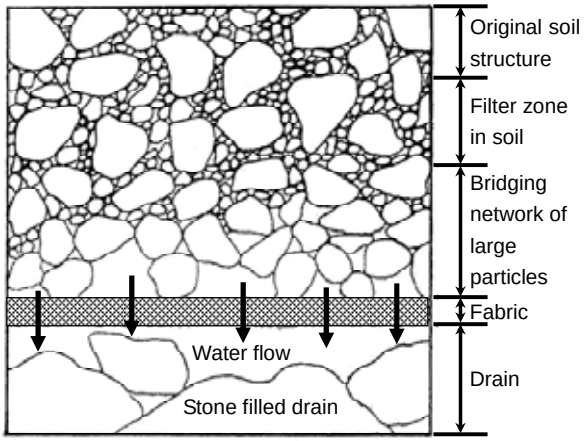

Fig. 1 Bridging network formations (Rollin and Lombard, 1988)

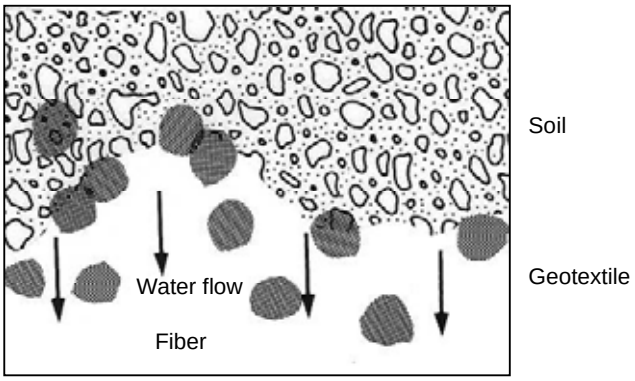

Fig. 2 Vault network formations (Rollin and Lombard, 1988)

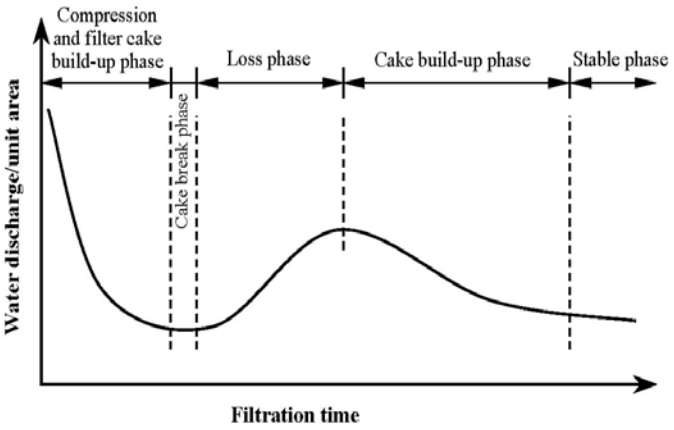

Fig. 3 Typical mechanisms of flux decay of a system (Mlynarek et al., 1991).

Fig. 4 Photo of cyclic flow apparatus (Ho, 2007)

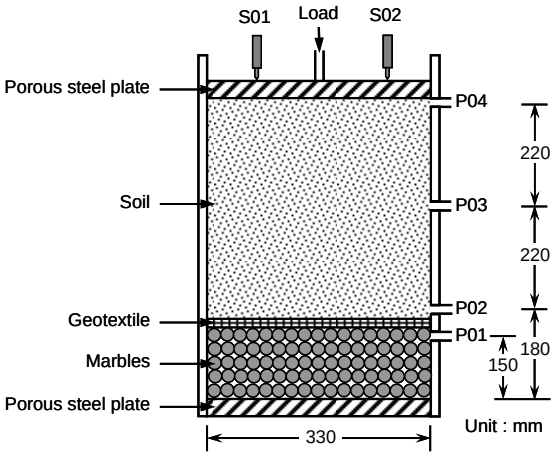

Fig. 5 Detailed schematic view of the internal setup of chambers (Chen *et al.*, 2008)

4. TEST MATERIALS

In order to understand the effect of fine soil content on the filtration behavior of geotextile, one geotextile together with seven soil compositions is studied. Their engineering properties are described below.

4.1 Soils

The soil tested is composed of various weight proportions of sand, silt and clay. The sand is Vietnam sand, classified as *SP* (poorly-graded sand) based on the Unified Soil Classification System (USCS). The properties of this sand are: specific gravity $G_s = 2.66$, maximum void ratio $e_{max} = 0.76 \sim 0.77$, and minimum void ratio $e_{min} = 0.56 \sim 0.57$. In order to avoid the influence of the fines in original sand, the soil was washed and filtered out the fines smaller than 0.074 mm before testing.

The silt soil was obtained from an alluvial soil of Xindian Creek. This alluvial soil was air-dried at first, and coarse particles larger than 0.074 mm were filtered out by sieves. The collected fine particles were then mixed with water and left for sedimentation. After the slurry dried out, the non-cohesive soil remaining at the bottom was the silt for testing. The classification of this silt is *ML*.

The clay soil was sampled from the sediment of Keelung River. The sediment soil was pretreated following the same way as mentioned above. However, the cohesive soil was the soil floating at top.

Seven soil specimens were prepared by weight; their components, soil classification symbols, and hydraulic conductivities are tabulated in Table 1. For the mixtures of G-01 to G-05, the percentage of silt content increases from 0% to 20%. For G-06 and G-07, the amount of fines content (less than 0.074 mm) is 10%. However, G-06 contains 6.5% silt and 3.5% clay; and G-07 contains 3.5% silt and 6.5% clay. As can be seen, the hydraulic conductivity reduces as the fines content and the clay amount increase.

Table 1 The proportions of soil specimens

Test No.		Vertical Pressure (kPa)	Sand (%)	Silt (%)	Clay (%)	Classification (USCS)	Conductivity k_s (cm/s)
G-01	a	70	100	0	0	*SP*	4.38×10^{-2}
	b	140					
G-02	a	70	95	5	0	*SP*	3.25×10^{-3}
	b	140					
G-03	a	70	90	10	0	*SP-SM*	1.43×10^{-3}
	b	140					
G-04	a	70	85	15	0	*SM*	8.33×10^{-4}
	b	140					
G-05	a	70	80	20	0	*SM*	4.38×10^{-4}
	b	140					
G-06	a	70	90	6.5	3.5	*SP-SM*	8.41×10^{-4}
	b	140					
G-07	a	70	90	3.5	6.5	*SP-SC*	7.22×10^{-5}
	b	140					

The particle size distributions of seven specimens are shown in Fig. 6; the characteristic particle sizes are expressed in Table 2. Because the parts of larger particle distributions of seven specimens are about the same, only the parts less than 30% passing are shown. From G-01 to G-05, the average particle diameter, d_{50}, and the effective grain size, d_{10}, decrease. Bhatia and Huang (1995) suggested that soils with values of coefficient of curvature above 7 should be considered as internally unstable and below this value internally stable. As can be seen from Table 2, the coefficients of curvature of all specimens are less than 7; consequently, they are considered as internally stable. In addition, the geometrical stability of soil was evaluated using the criterion proposed by Kenney and Lau (1985), which is based on a method of describing the shape of grain-size distribution. The increment of percent passing (H) that occurs over a designated grain size interval of d to $4d$ is compared to the percent passing (F) at grain size d. A boundary defined by a stability index, $H/F = 1.0$, is for separating unstable soils from stable soils. According to the result analyzed by this method (Fig. 7), all specimens except G-06 are stable. However, these specimens will be further investigated regarding the stabilities of soil-geotextile filter systems under cyclic flow conditions.

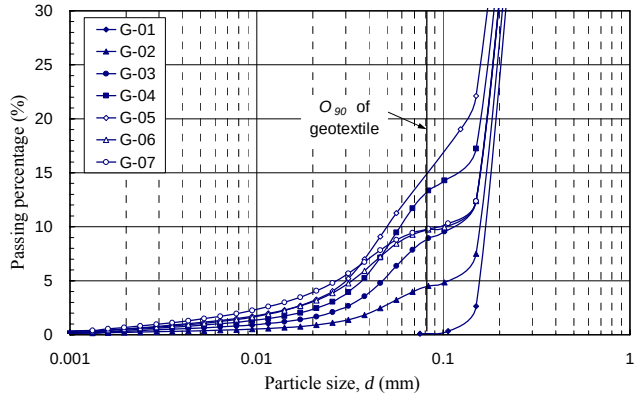

Fig. 6 Particle size distributions of test specimens

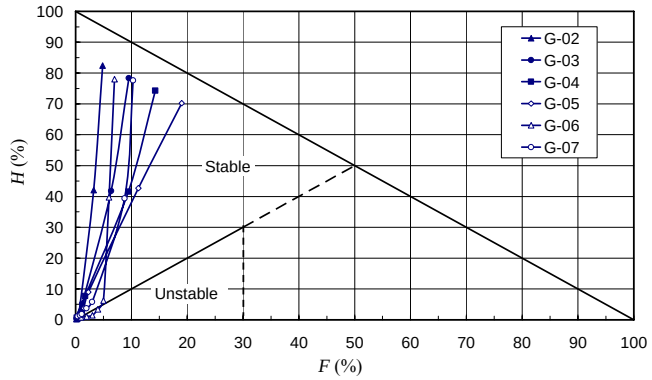

Fig. 7 The result of analysis of the internal stability of soil filter by the criterion of Kenney and Lau (1985)

Table 2 The characteristic values of soil specimens

Test No.	d_{10} (mm)	d_{15} (mm)	d_{30} (mm)	d_{40} (mm)	d_{50} (mm)	d_{60} (mm)	d_{85} (mm)	d_{90} (mm)	C_u	C_c	I_p
G-01	0.180	0.180	0.210	0.240	0.270	0.302	0.408	0.470	1.7	0.8	–
G-02	0.170	0.170	0.204	0.230	0.265	0.298	0.402	0.466	1.8	0.8	–
G-03	0.110	0.150	0.200	0.215	0.255	0.285	0.400	0.452	2.6	1.3	–
G-04	0.059	0.115	0.181	0.209	0.240	0.280	0.392	0.447	4.7	2.0	–
G-05	0.048	0.082	0.176	0.200	0.230	0.275	0.388	0.438	5.7	2.3	–
G-06	0.105	0.150	0.200	0.215	0.255	0.285	0.400	0.452	2.7	1.3	–
G-07	0.092	0.150	0.200	0.215	0.255	0.285	0.400	0.452	3.1	1.5	5

Note: d_x = soil particle size corresponding to percent passing; C_u = coefficient of uniformity; C_c = coefficient of curvature; I_P = plasticity index.

4.2 Geotextile

With regard to the geotextile for testing, Hoare (1984) proposed to adopt thin heat-bonded geotextiles for unidirectional flow conditions and thick needle-punched geotextiles for cyclic flow conditions. On the other hand, Giroud *et al.* (1998) suggested that a two-layer nonwoven geotextile is suitable for protecting river or coastal revetment. In view of this, this study employed a thick two-layer needle-punched geotextile for a series of tests; the relevant properties of the geotextile are given in Table 3.

Table 3 The properties of the geotextile

Properties and testing method	Unit	Symbol	Value
Characteristic opening size based on hydrodynamic sieving, EN ISO 12956	mm	O_{90}	0.08
Hydraulic conductivity normal to the plane, EN ISO 11058	cm/s	k_g	6.0
Elongation, EN ISO 10319	%	ε_{max}	85
Tensile strength, EN ISO 10319	kN/m	T_{max}	23
Mass per unit area, DS EN 965	g/m^2	μ_A	400
Thickness, DS EN 964-1 (2 kPa)	mm	t_{GTX}	3.5

4.3 Examination of Test Materials

For cyclic flow conditions, Schober and Teindl (1979) suggest that the coefficient of hydraulic conductivity of geotextile must be greater than that of soil. The Federal Waterways Engineering and Research Institute in Germany (BAW, Bundesanstalt für Wasserbau, 1993) proposes

$$k_g \geq 10\, k_s \quad \text{for non-cohesive soil} \tag{1}$$

$$k_g \geq 100\, k_s \quad \text{for cohesive soil} \tag{2}$$

where k_g and k_s are the hydraulic conductivities of geotextile and soil, respectively. Since the coefficient of hydraulic conductivity of tested geotextile, k_g, is 6.0 cm/s and according to the permeability of each specimen listed in Table 1, it is apparent that the geotextile satisfies the permeability requirement for all soil specimens. Moreover, a good soil-geotextile filter system needs also satisfy the retention criteria listed in Table 4. For this examination, the parameters shown in Table 2 are used. The result of each specimen also satisfies the retention criteria.

Table 4 The retention criteria for soils under cyclic flow condition

References	Base soil type	Retention criterion
Heerten (1982)	non-cohesive soil	$O_{90} < d_{50}$
	cohesive soil	$O_{90} < 10\, d_{50}$ and $O_{90} \leq d_{90}$ and $O_{90} \leq 100$ μm
ASPG (1985)	$d_{40} > 60$ μm	$O_{90} \leq 1.5\, d_{10}\,(C_u)^{1/2}$ and $O_{90} \leq d_{60}$
CFGG (1986)	loose sand ($C_u > 4$)	$O_{90} < 0.6\, d_{85}$
	loose sand ($C_u \leq 4$)	$O_{90} < 0.48\, d_{85}$
DGEG (1986)	$d_{40} > 60$ μm	$O_{90} < d_{90}$
PIANC (1987)	$C_u > 5$	50 μm $< O_{90} < d_{90}$
	$C_u < 5$	50 μm $< O_{90} < 0.7\, d_{90}$
Młynarek (2000)	$d_{50} \geq 75$ μm and $C_u < 6$	$O_{90} < 0.8\, d_{50}$ or 150 μm $< O_{90} < d_{50}$

5. TEST PROCEDURE

To investigate the effect of overburden pressure on the filtration function of geotextile under cyclic flow, the specimens were subject to loadings of 70 kPa and 140 kPa, respectively. In addition, the wave period applied ranged from long to short periods, *i.e.*, 600, 300, 150, and 75 seconds, respectively. The testing procedure is summarized briefly as follows:

1. After the apparatus had been set up, the test soil at optimum water content was divided into eight layers of equal weight and placed in the upper chamber. Each layer of soil was compacted until it reached the maximum dry density. With these eight layers, the total height of the soil specimen was 45 cm. The maximum dry density and the optimum water content were obtained by the Standard Proctor Compaction Test (ASTM D698). The test results are shown in Fig. 8. However, the pure sand specimen, G-01, was prepared with the relative density equal to 88%.

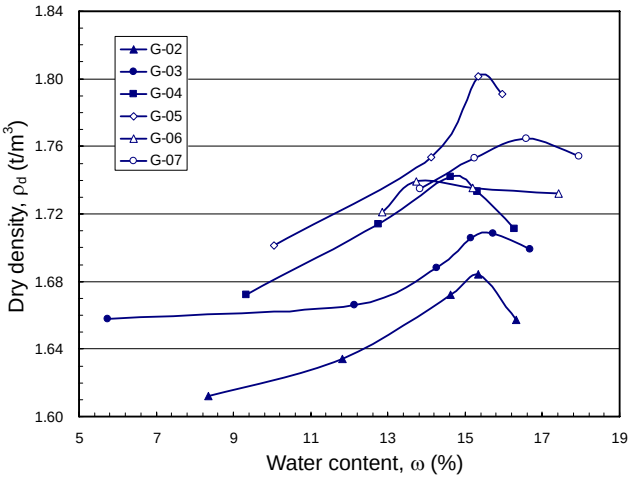

Fig. 8 Standard Proctor compaction curves

2. The specimen was then saturated with water gradually from the bottom until water reached the top of the specimen. This procedure repeated three times in order to ensure full saturation. Alternatively, pore pressures recorded by four transducers were compared with the elevation of piezometers, used as a check to examine whether the specimen was fully saturated.
3. The loading device was fixed to the chamber and normal pressure was applied in the increments of 10 ~ 20% of maximum normal load. A subsequent increment of loading was added only after the settlement induced by previous loading had become very small and when the pore-water pressure was equal to the static water pressure measured by the piezometers.
4. Under constant normal pressure, 70 kPa or 140 kPa, the specimen was then subjected to cyclic flows in the order of 600, 300, 150 and 75 sec/cycle of wave period, respectively. The test duration for each constant period was at least 48 hours until the variation in pore-water pressure became stable.
5. During testing, pore-water pressures at different positions were recorded automatically by piezometers; and the settlement at the top of specimen was monitored by settlement gages.
6. After the test was finished, soil samples were taken at different locations for investigation of the variation in grain size distribution. Moreover, a stereomicroscope was utilized to observe the inside condition of the geotextile.

6. TEST RESULTS

As stated above, pore-water pressures at various levels in the specimen were recorded in order to examine the phenomena such as clogging, blocking, or boiling that might occur in a filtration system. The measured settlement can also be compared with the pore-water pressure to find out if there exists a relationship between them.

6.1 Pore-Water Pressure

Figure 9 shows the pore-water pressure response of pure sand, G-01, at wave periods of 600 and 150 sec/cycle, respectively. The peak pore-water pressure increases as the wave period decreases. This is because pore-water pressure has not dissipated completely when the next cycle of flow comes up in the cases of shorter period flows. For pure sand under various normal stresses, the difference in pore pressure is not significant. This implies that pure sand has an incompressible and porous structure to restrain soil particles from migrating under the action of normal pressure. Furthermore, the pore-water pressures of P01 and P02 are about equal, indicating no clogging or blocking within the geotextile.

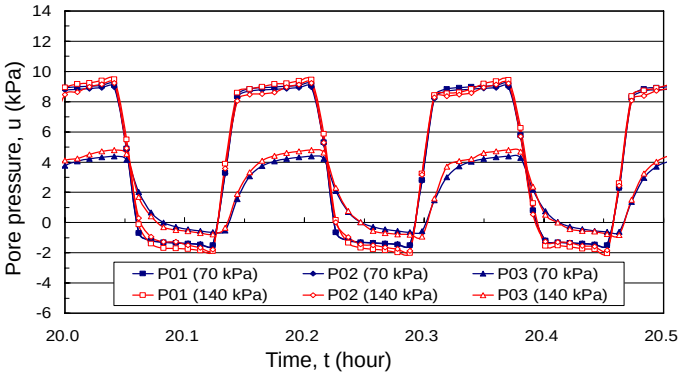

(a) 600 sec/cycle

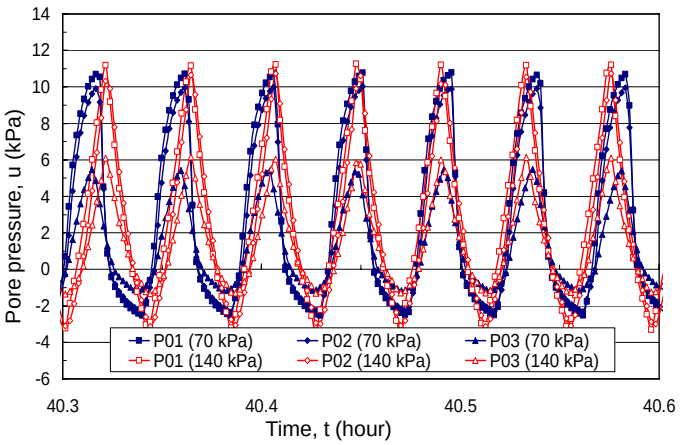

(b) 150 sec/cycle

Fig. 9 Pore-water pressure of pure sand (G-01)

A phenomenon is noteworthy for G-02-b under the wave period of 300 sec/cycle, *i.e.*, the pore-water pressure response was not uniform during testing (see Fig. 10); it decreased with time for several hours and then remained stable. This specimen, G-02, contains only 5% silt; the fines in voids were probably not enough to form a dense structure even under a high normal pressure. Consequently, the pore-water pressure increased gradually in the beginning, but once it reached a certain value the fines then started to migrate. At some locations where there was significant loss of fines, local soil boiling might occur. In the mean time, loss of fines also increased the hydraulic conductivity of soil and decreased pore-water pressure. The same phenomenon can also be found in specimen G-03-a, though it contains more silt, 10%. In this case, boiling phenomenon was owing to the specimen subjected to a low normal pressure. In other words, the normal pressure was not high enough to impede fines to move.

Figures 11 and 12 present the pore-water pressure response for silty sand specimens, G-03 and G-04, under the wave periods of 600 sec/cycle and 150 sec/cycle, respectively. They illustrate that fines content may cause the peak pore-pressure to increase. As to the effect of wave period, pore-water pressure in long period condition has enough time to transmit, hence is lower than that in short period condition. Moreover, it is obvious that normal pressure affects pore-water pressure as well; higher normal pressure induces a higher response. This is because not only fine particles affect the response but also they are more susceptible to form a denser structure when under load.

For specimens G-04 and G-05 that contain 15% and 20% of silt, respectively, the soil structures tend to be more stable. Therefore, the amplitudes of pore-water pressure are uniform, as local soil boiling phenomenon was not observed during testing. It seems that silt content of 10% is approximate the threshold value for local boiling to occur.

The effect of clay content upon pore-water pressure can be seen from Fig. 13. Figure 13(a) shows the variation in pore-water pressure for specimen G-06 under 150 sec/cycle of wave period. Comparing Fig. 13(a) with Fig. 11(b), specimen G-06 having 3.5% of clay content results in higher response of pore pressure than G-03-b.

Figure 13(b) shows the variation in pore-water pressure for G-07 under wave period of 150 sec/cycle. The peak pore-water pressure of G-07 is also higher than that of G-06. It is understandable that the reason is more clay content in G-07. Moreover, there was no local boiling in the process of testing G-07, as clay has cohesion to limit soil migration. Thus, clayey soil will not only reduce the potential of local boiling but also increase the pore-water pressure response.

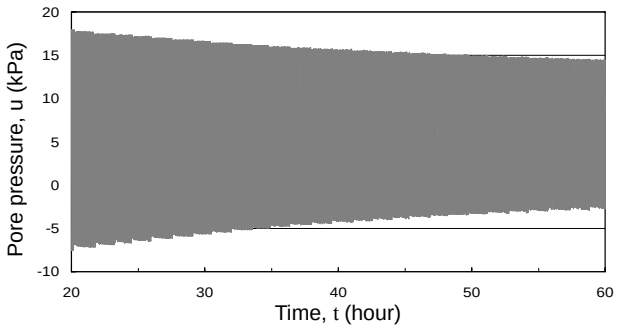

Fig. 10 Envelope of peak pore pressure (P02) of G-02-b under 300 sec/cycle of wave period

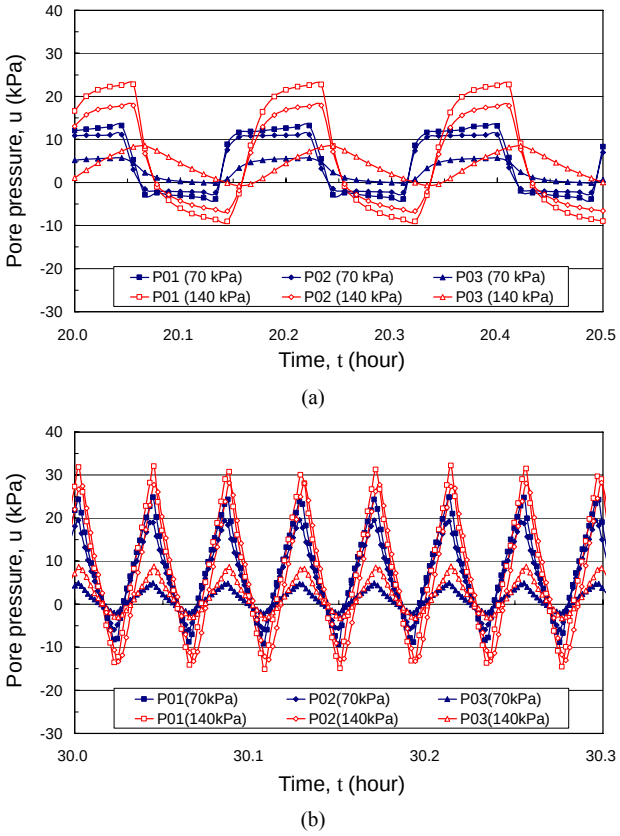

Fig. 11 Pore-water pressure of silty sand (G-03): (a) 600 sec/cycle; (b) 150 sec/cycle

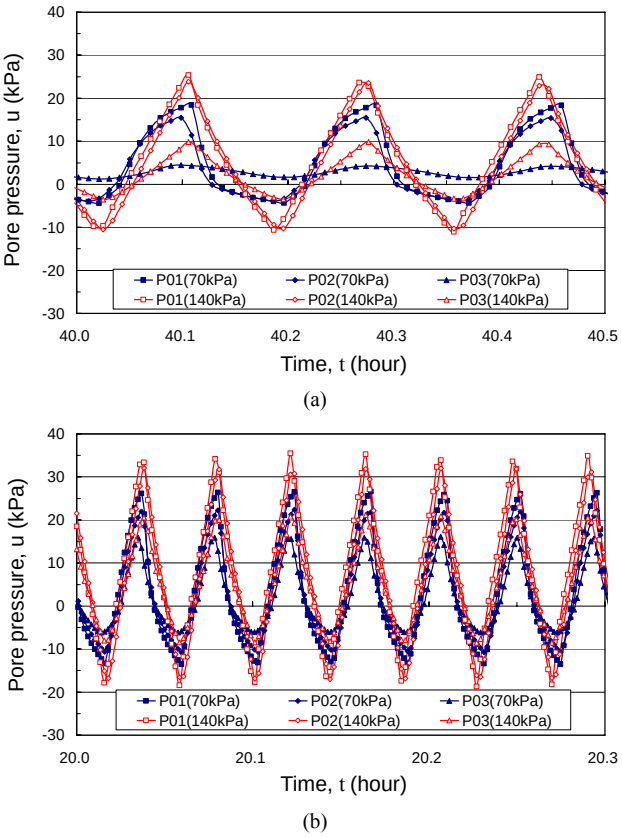

Fig. 12 Pore-water pressure of silty sand (G-04): (a) 600 sec/cycle; (b) 150 sec/cycle

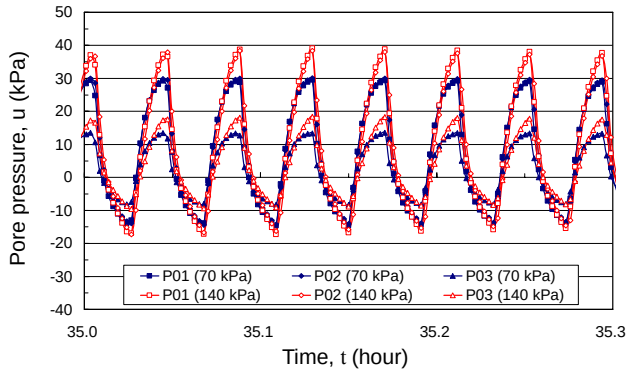

(a)

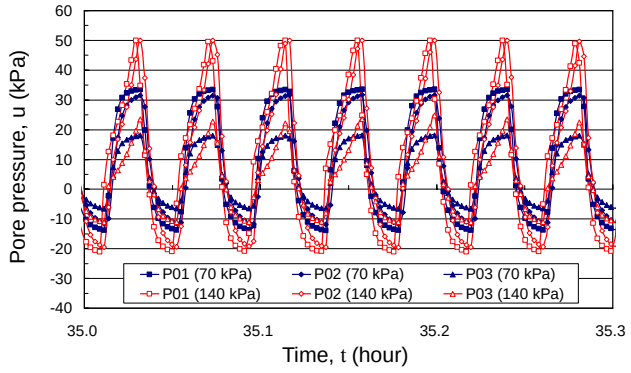

(b)

Fig. 13 Pore-water pressure of clayey-silty sand (at 150 sec/cycle of wave period): (a) G-06; (b) G-07

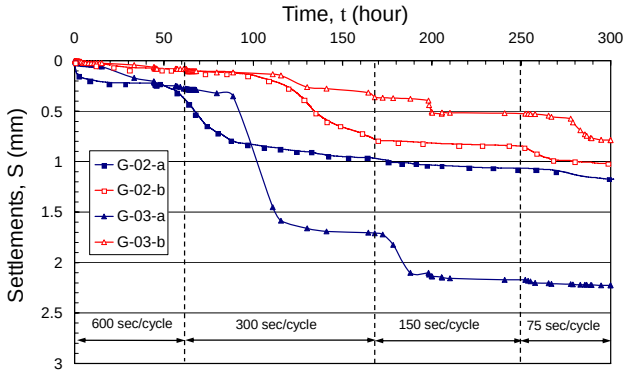

(a)

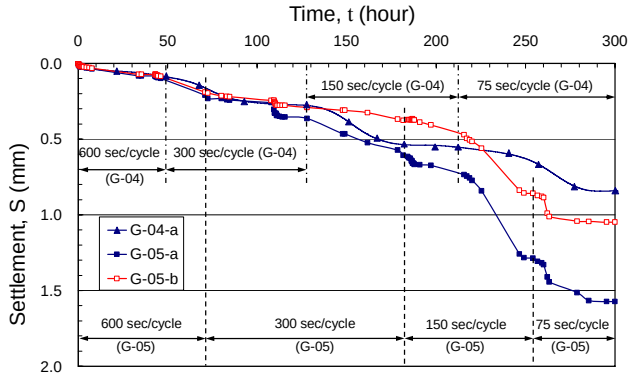

(b)

Fig. 14 Settlement curves of silty sand: (a) G-02 and G-03; (b) G-04 and G-05

6.2 Settlement

The settlement curves of pure sand (G-01, not shown) are virtually the same irrespective of normal pressures. As discussed previously, the difference in pore-water pressure for pure sand under different normal pressures is negligible. It can thus be concluded that sand can form a structure that particles are not able to move easily under cyclic flows; consequently, the settlement is insignificant.

Figure 14(a) presents the settlement curves of silty sand specimens under different normal pressures. The settlement under 140 kPa is less than that under 70 kPa, arising from a higher stress between particles inducing a denser structure as well as preventing particles from moving. In particular, for G-02-a, G-02-b and G-03-a, the settlements increase dramatically during the action of wave period at 300 sec/cycle. Compared with pore pressure response (*e.g.*, Fig. 10), it is obvious that pore pressure reduces as settlement occurs. This is because an upward flow increases pore pressure and reduces the effective stress in the soil small enough that coarse and fine particles can separate and migrate away from the geotextile, *i.e.*, a local boiling. As water flows downwards again, soil particles migrate towards the geotextile and some fines passing through the geotextile are collected in the wash-out tank.

Furthermore, soil boiling causes fines to suspend on coarse particles. As water flows downwards, heavier coarse particles precipitate relatively fast than fines. In this situation, rearrangement of soil particles is so significant that a sudden settlement occurs until a stable soil structure is formed. After the soil structure becomes stable, settlement will tend to mitigate. For this reason, soil boiling is one of the important factors that cause settlement. In addition, comparing the curves of G-04-a and G-05-a in Fig. 14(b), the settlement increases with increasing amount of silt because silt is cohesionless thus apt to be washed away.

The variation in settlement for clayey-silty sand is shown in Fig. 15. From the settlement curves of G-06-a and G-07-a, it is not surprising that more clay content will combine soil particles effectively and prevent soil boiling from happening. The other reason is that the dry density of G-07 is higher than that of G-06 (Fig. 8); hence a denser structure has a less tendency of boiling.

In conclusion, the above results show that overburden pressure as well as soil composition play important roles in the settlement behavior of a soil-geotextile filtration system.

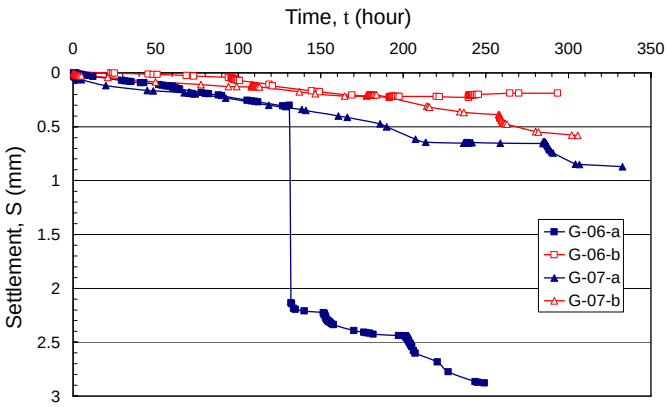

Fig. 15 Settlement curves of clayey-silty sand

6.3 The Change in the Amount of Fine Soils

In order to justify the mechanism mentioned above, some soils are taken from three positions in the chamber to evaluate their particle size distributions. The top position is above the soil boiling zone; the middle position is within the soil boiling zone; and the bottom position is in the vicinity of the geotextile. Table 5 shows the amount of fines smaller than 0.074 mm before and after testing. It can be seen that the percentages of fines in all specimens have changed after testing. At the bottom position, some fines are washed away or moved to other places; therefore, the fines content decreases after testing. Generally speaking, at the middle and bottom positions the fines content reduces more for lower normal pressure, except for G-07-a and G-07-b at middle positions. Moreover, soil boiling makes fines move upwards; hence the fines content increases at the top position and decreases at the middle position. For cases where no soil boiling occurs, the change in the fines content is not significant at both the top and middle positions. It is clear that soil boiling is the main cause of a significant settlement when the specimen has small amount of silt and subjected to low normal pressure.

Table 5 The percentage of fine particle (d < 0.074 mm) at different positions after testing

Test No.		Normal pressure (kPa)	Soil boiling	Fine particle content (%)			
				Before testing	After testing		
					Top	Middle	Bottom
G-02	a	70	Yes	5	7.29	4.03	3.94
	b	140	Yes	5	6.26	5.11	4.07
G-03	a	70	Yes	10	11.74	6.63	4.01
	b	140	No	10	9.63	8.93	8.12
G-04	a	70	No	15	15.89	14.51	11.61
	b	140	No	15	15.47	15.49	14.35
G-05	a	70	No	20	22.14	19.26	17.77
	b	140	No	20	21.08	20.44	18.47
G-06	a	70	Yes	10	10.68	5.24	5.15
	b	140	No	10	9.84	9.56	8.44
G-07	a	70	No	10	9.97	9.59	8.82
	b	140	No	10	10.09	9.42	9.07

Table 6 The mass of soil wash-out per unit area (unit: g/m^2)

Test No.	Fines content (%)		Normal pressure (kPa)	
	Silt	Clay	70	140
G-01	0	0	79.6	63.2
G-02	5	0	421.0	352.2
G-03	10	0	5096.1	490.6
G-04	15	0	4351.6	513.6
G-05	20	0	5517.5	570.4
G-06	6.5	3.5	389.3	409.2
G-07	3.5	6.5	486.4	465.2

6.4 Soil Wash-Out

After testing, the soil wash-out is collected and the amount per square meter is shown in Table 6. For pure sand, G-01, there are only small amounts of soil collected under various normal pressures. For G-03-a, G-04-a and G-05-a, much more soil are collected under low normal pressure in comparison to high normal pressure due to small effective stress having difficulty in confining particles effectively. Lafleur *et al.* (1989) defined a threshold value, 2500 g/m^2, to distinguish stable and unstable filtration systems for base soil. As stated previously, soil boiling occurs in G-03-a. In this situation, silt soil disperses in the water and moves more easily; hence particle rearrangement and soil loss are the primary causes of the settlement in this case.

The effect of clay content on soil wash-out behavior is obvious, as can be seen from comparing the results of G-03, G-06, and G-07. Though all three specimens having the same fines content, 10%, the wash-out collected from G-03 is much more. Apparently, this again is due to the effect of clay content which prevents soil boiling from occurring in specimens G-06 and G-07.

6.5 Summary

According to the results discussed above, a summary is made. For pure sand specimen, G-01, it contained no fines and large particles formed a porous structure that water flew easily within the soil under cyclic flow action. Consequently, the variation in pore-water pressure was regular; the settlement was small; and the least amount of soil was collected. For specimens G-04 and G-05 that contain more than 10% of silty soil, no local soil boiling were found due to their stable soil structures (C_u > 4 and C_c = 1 ~ 3). In addition, the test result of specimen G-07 also shows that the soil structure is stable (C_u > 3 and C_c = 1 ~ 3).

The characteristics of soil specimens that have boiling phenomenon are presented in Table 7. The silt contents in these specimens are 5 ~ 10%. These specimens have no plasticity and are classified as *SP* and *SP-SM*.

As stated previously, Bhatia and Huang (1995) suggested soils with C_u < 7 should be considered as internally stable. As can be seen from Table 7, the C_u values range from 1.8 ~ 2.7 and C_c values are 0.8 ~ 1.3. In addition to that, all these specimens satisfy the criteria listed in Table 4. However, soil boiling still occurred in some conditions, particularly under low normal pressure as presented in Table 7. In view of this, the design criteria for some soils under cyclic flow condition should be examined more carefully and take into account the key factors such as silt content, grain size distribution, and in-situ overburden pressure, *etc*.

Table 7 The characteristics of soil specimens with boiling phenomenon

Test No.		Normal Pressure (kPa)	Silt (%)	Clay (%)	Classification (USCS)	C_u	C_c	I_p
G-02	a	70	5	0	*SP*	1.8	0.8	none
	b	140						
G-03	a	70	10	0	*SP-SM*	2.6	1.3	none
G-06	a	70	6.5	3.5	*SP-SM*	2.7	1.3	none

7. MICRO-OBSERVATION OF GEOTEXTILES

After testing, a stereomicroscope is utilized to observe the clogging condition in the geotextile. Figure 16 shows the surface of the geotextile after testing. As can be seen, the areas where marbles locate are darker. In order to look into details, two pieces of geotextiles are cut for observance by a stereomicroscope.

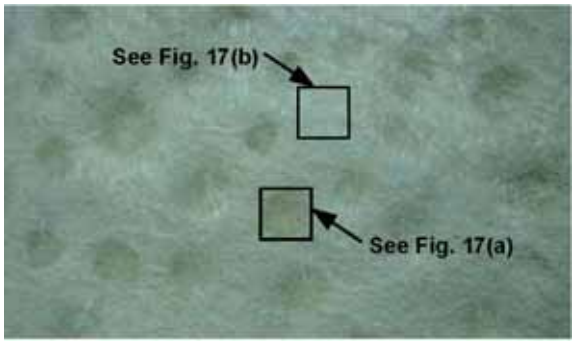

Fig. 16 Two surface conditions of geotextile after testing (G-04-a)

Figure 17(a) shows the micro phenomenon of the geotextile surface that contacts with marbles, and it is easy to see fine soils adhered to fibers. Figure 17(b) shows the area between marbles, and only a few particles are visible in this clean area.

To explain the two different behaviors, schematic drawings are made in Fig. 18. When the water flows downwards, soil particles migrate towards the geotextile with some fines clogged within the geotextile and some passing through the geotextile (see Fig. 18(a)). As the water flows upwards, it will pass through fibers and take away the fines that clogged within the geotextile, but the particles behind the marbles are difficult to be removed by the upward flow (Fig. 18(b)). This phenomenon will take place as cyclic flow continues until a stable soil-geotextile filtration system is established.

In order to observe the surface condition of geotextile and to examine the soil structure, a soil-geotextile sample is taken carefully from an area between marbles. In Fig. 19, a bridging network is found forming adjacent to the geotextile. In this area, most particles have been washed away and a hollow space is thus generated. According to this observation, a network is able to form under long-term cyclic flow. The network prevents soil erosion and further settlement. This finding is not the same as what Giroud (1982) and Köhler (1993) proposed that a bridging network is unable to form under short-term cyclic flow.

Moreover, Fig. 20 shows the micro phenomenon of the cross sections of geotextile after testing specimens G-3-a, G-6-a, and G-7-a. These three soils contain 10% of fines, but have different clay contents, 0%, 3.5%, and 6.5%, respectively. Their micro phenomena are quite different. For G-03-a, the fine particles adhere to fibers is less than G-06-a and G-07-a. This can be explained that most fine particles clogged within the geotextile are eroded due to soil boiling, as more settlement and wash-out are found in comparison with the other two. On the contrary, G-07-a containing more clay has more fine particles adhered to fibers. This phenomenon reduced the voids of geotextile and increased pore-water pressure. This is the reason why the pore-water pressure of G-07-a is higher than those of G-06-a and G-05-a under the same wave period condition.

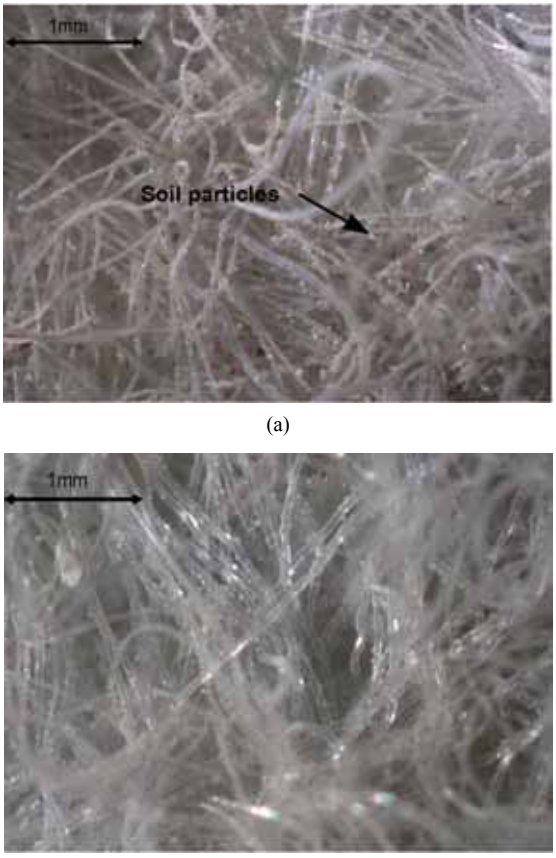

Fig. 17 The surface conditions of geotextile (magnification ratio: 25) (G-04-a): (a) the area contacting with marbles; (b) the area between marbles

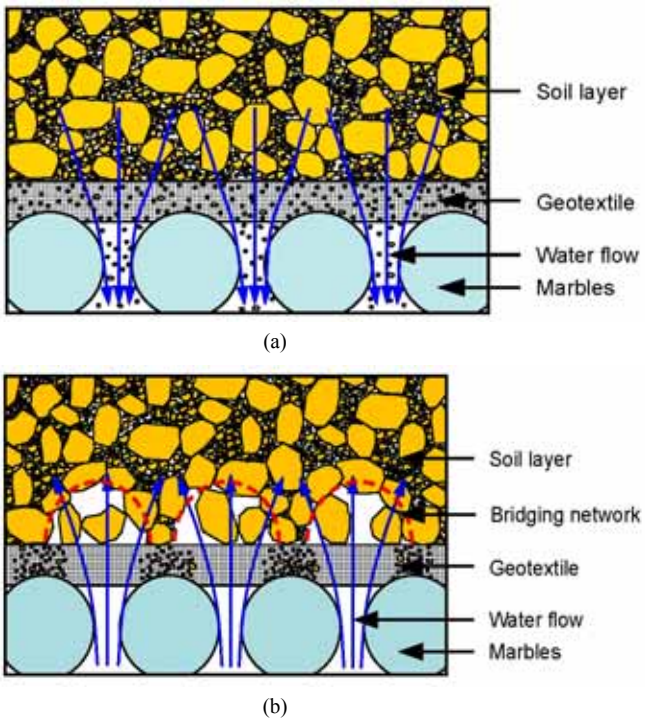

Fig. 18 Schematic migration of fine particles under cyclic flows: (a) downwards flow; (b) upwards flow

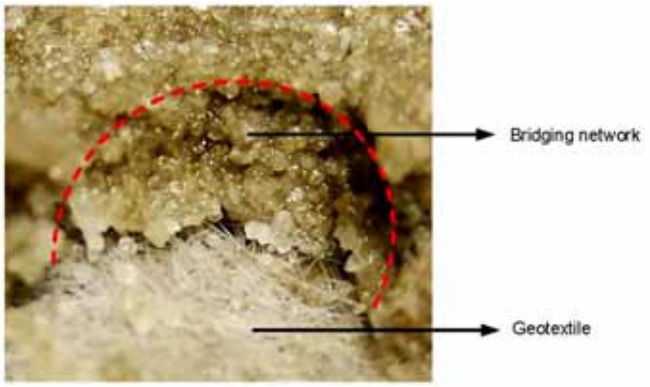

Fig. 19 A bridging network formed adjacent to geotextile (G-06-a)

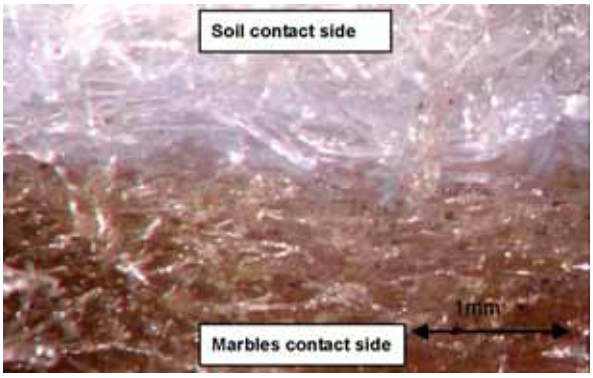

(a)

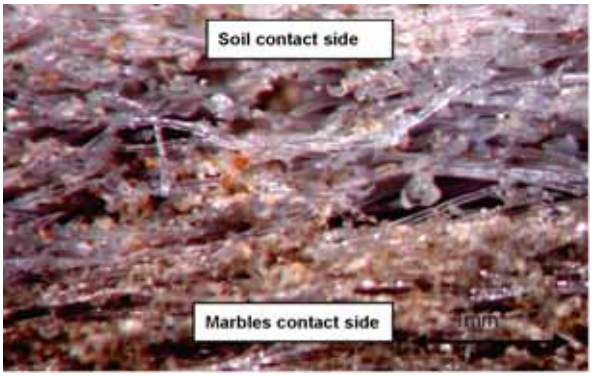

(b)

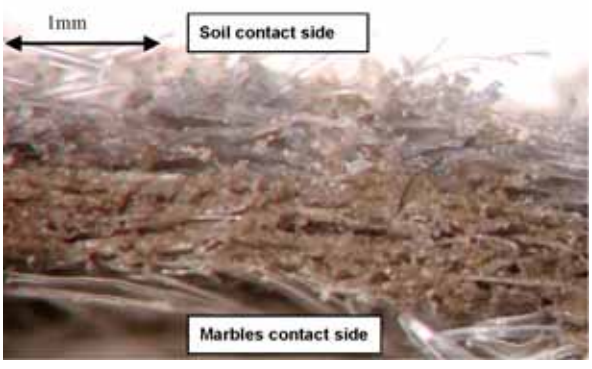

(c)

Fig. 20 Micro photos of the cross sections of geotextile (magnification ratio: 25): (a) G-03-a; (b) G-06-a; (c) G-07-a

8. CONCLUSIONS

This paper presents the investigation on soil-geotextile filtration mechanisms under long-term cyclic flows using a self-developed apparatus. The soil samples are composed mainly of sand, with 0 ~ 20% fines content of silt and clay. The factors taken into account are the effect of overburden pressure and cyclic flow periods ranging from long to short, in order to simulate a range of waves. After testing, a stereomicroscope is utilized to observe the microstructure of the geotextile filter. The results from this study are summarized as follows:

1. For the same soil specimen, the peak pore-water pressure increases as the cyclic flow period decreases. The peak pressure also increases with the amount of cohesive soil in the specimen. This is due to the low hydraulic conductivity of cohesive soil as well as the excess pore-water pressure has no enough time to dissipate in a short period.
2. The structure of pure sand is relative stable under various normal pressures. In consequence, the difference in pore-water pressure, settlement, and the amount of soil loss are insignificant.
3. For silty sands having 10-20% silt, low normal pressure could not confine the cohesionless particles effectively. Under these conditions, the particles in the specimens of G-03-a, G-04-a, and G-05-a were easily washed away and caused significant soil loss. However, some clay content in the specimens, such as G-06-a and G-07-a, as well as higher normal pressure reduced soil loss significantly.
4. Boiling phenomenon occurred in specimens that have silt content less than 10%. Soil boiling induced a sudden settlement, but it did not cause so much soil loss as induced in specimens with 10-20% silt content.
5. The micro phenomenon observed by the stereomicroscope showed that a bridging network was able to form under long-term cyclic flow. This network can prevent soil erosion and further settlement.
6. Boiling phenomenon occurred in some conditions, particularly under low normal pressure. Hence, the design criteria for certain kinds of soils under cyclic flow condition should be examined more carefully. The key factors such as silt content, grain size distribution, and in-situ overburden should be taken into consideration.

ACKNOWLEDGEMENTS

The financial support is provided by the National Science Council, ROC. Special thanks also go to Dr. Yves-Henri Faure, LIRIGM, UJF, Grenoble, France for generously supplying the geotextile and offering valuable suggestions.

NOTATIONS

Basic SI units are given in parentheses.

C_c coefficient of curvature (dimensionless)
C_u coefficient of uniformity (dimensionless)
d soil particle size (mm)
d_x soil particle size corresponding to x percent passing (mm)

d_{10} effective grain size (mm)
d_{50} average particle diameter (mm)
e_{max} maximum void ratio (dimensionless)
e_{min} minimum void ratio (dimensionless)
F passing percentage of soil at grain size d (%)
G_s specific gravity of soil (dimensionless)
H increment of passing percentage of soil for grain size interval of d to 4d (%)
I_P plasticity index (dimensionless)
k_g hydraulic conductivity of geotextile normal to the plane (m/s)
k_s hydraulic conductivity of soil (m/s)
O_{90} geotextile characteristic opening size based on hydrodynamic sieving. (mm)
ML low plasticity silt
S settlement (mm)
SM silty sand
SP poorly-graded sand
SP-SC poorly graded sand with clay
SP-SM poorly graded sand with silt
T_{max} tensile strength of geotextile (kN/m)
t time (hour)
t_{GTX} thickness of geotextile (mm)
u pore-water pressure (kPa)
ε_{max} elongation of geotextile (%)
ρ_d dry density (t/m^3)
μ_A mass per unit area of geotextile (g/m^2)
ω water content

ABBREVIATIONS

ASPG Swiss Association of Professional on Geotextiles
CFGG French Committee on Geotextiles
DGEG Germany Committee of Soil Mechanics and Foundations Engineering
LVDT linear variable differential transformer
PIANC Permanent International Association of Navigation Congresses
USCS Unified Soil Classification System

REFERENCES

ASPG (1985). *The Manual of the Geotextiles – Resistance to the Opening Size O_d.* Association Suisse des Professionnels de Géotextiles (Swiss Association of Professionals on Geotextiles), Zurich, Switzerland (in French).

ASTM D 698-07e1. "Stand test methods for laboratory compaction characteristics of soil using standard effort (12,400 ft-lbf/ft^3 (600 kN-m/m^3))." *ASTM International*, West Conshohocken, PA, USA.

Aydilek, A. H. (2006). "A semi-analytical methodology for development of woven geotextile filter selection criteria." *Geosynthetics International*, **13**(2), 59–72.

BAW - Bundesanstalt für Wasserbau (1993). "Code of practice for the use of geotextile filters on waterways." *The Federal Waterways Engineering and Research Institute in Germany,* Karlsruhe.

Bhatia, S. K. and Huang, Q. (1995). "Geotextiles filters for internally stable/unstable soils." *Geosynthetics International*, **2**(3), 537–565.

Cazzuffi, D., Mazzucato, A., Moraci, N. and Tondello, M. (1999). "A new test apparatus for the study of geotextiles behavior as filters in unsteady flow conditions: relevance and use." *Geotextiles and Geomembranes*, **17**(5-6), 313–329.

CFGG (1986). AFNOR G38017, *Association Française de Normalisation* (French Committee on Geotextiles), La Plaine Saint-Denis, France (in French).

Chen, R. H. and Chen, C. N. (1986). "Permeability characteristics of prefabricated vertical drains." *Proceedings of the 3rd International Conference on Geotextiles*, Vienna, Austria, **3**, 785–790.

Chen, R. H., Ho, C. C. and Hsieh, A. T. (2006). "Filtration behavior of geotextile under normal pressure and bi-directional cyclic flow." *Proceedings of the 8th International Conference on Geosynthetics*, Yokohama, Japan, **2**, 557–560.

Chen, R. H., Ho, C. C. and Hsu, C. Y. (2008). "The effect of soil fines content on the filtration characteristics of geotextile under cyclic flows." *Geosynthetics International*. **15**(2), 95–106.

Chew, S. H., Tian, H., Tan, S. A. and Karunaratne, G. P. (2003). "Erosion stability of punctured geotextile filters subjected to cyclic wave loadings—A laboratory study." *Geotextiles and Geomembranes*, **21**(4), 221–239.

DGEG (1986). "Use and examination of civil engineering and hydraulic engineering." *Germany Committee of Soil Mechanics and Foundation Engineering*, Series of publications of the DVWK 76, Hamburg, German.

DS EN 964-1 (1996). "Geotextiles and geotextile-related products—Determination of thickness at specified pressures—Part 1: single layers." *Dansk Standard*, Charlottenlund, Denmark.

DS EN 965 (1996). "Geotextiles and geotextile-related products—Determination of mass per unit area." *Dansk Standard*, Charlottenlund, Denmark.

EN ISO 10319 (1993). "Geotextiles—Wide-width tensile test." *International Standardization Organization*, Geneva, Switzerland.

EN ISO 11058 (1999). "Geotextiles and geotextile-related products —Determination of water permeability characteristics normal to the plane, without load." *International Standardization Organization*, Geneva, Switzerland.

EN ISO 12956 (1999). "Geotextiles and geotextile-related products —Determination of the characteristic opening size." *International Standardization Organization*, Geneva, Switzerland.

Fannin, R. J. and Pishé, R. (2001). "Testing and specifications for geotextile filters in cyclic flow applications." *Proceedings of Geosynthetics 2001*, Portland, Oregon, U.S.A., 423–435.

Giroud, J. P. (1982). "Filter criteria for geotextiles." *Proceedings of the 2nd International Conference on Geotextiles*, Las Vegas, USA, 1, 103–108.

Giroud, J. P., Delmas, P. and Artières, O. (1998). "Theoretical basis for the development of a two-layer geotextile filter." *Proceedings of the 6th International Conference on Geosynthetics*, Atlanta, USA, **2**, 1037–1044.

Heerten, G. (1982). "Dimensioning the filtration properties of geotextiles considering long-term conditions." *Proceedings of the 2nd International Conference on Geotextiles*, Las Vegas, USA, **1**, 115–120.

Ho, C. C. (2007). *The Erosion Behavior of Revetment Using Geotextile*. Ph.D. Dissertation, National Taiwan University (Taiwan) and Joseph Fourier University of Grenoble (France).

Hoare, D. J. (1984). "Geotextiles as filter." *Ground Engineering*, **17**, 29-44.

Hsu, C. Y. (2007). "Filtration behavior of geotextile under bi-directional cyclic flow." *Master Thesis*, National Taiwan University (in Chinese).

Kenney, T. C. and Lau, D. (1985), "Internal stability of granular filters." *Canadian Geotechnical Journal*, **22**(2), 215–225.

Köhler, H. J. (1993). "The influence of hydraulic head and hydraulic gradient on the filtration process." *Proceedings of the 1st International Conference on Geofilters*, Karlsruhe, Germany, **2**, 225–240.

Lafleur, J., Mlynarek, J. and Rollin, A. L. (1989). "Filtration of broadly graded cohesionless soils." *Journal of Geotechnical Engineering*, ASCE, **115**(2), 1747–1768.

Lawson, C. R. (1982). "Filter criteria for geotextile: relevance and use." *Journal of the Geotechnical Engineering Division*, ASCE, **108**(10), 1300–1317.

Liao, H. J. and Chu, C. C. (2002). "The case study of backfill soil erosion in the tidal land of Taiwan." http://www.ceci.com.tw/book/53/ch53hp.htm, *CECI-Technology Magazine*, **53**, Taipei, Taiwan (in Chinese).

Luettich, S. M., Giroud, J. P. and Bachus, R. C. (1992). "Geotextile filter design guide." *Geotextiles and Geomembranes*, **11**(4-6), 355–370.

Młynarek, J. (2000). "Geodrains and geofilters—Retrospective and future trends." *Proceedings of the 3rd International Conference on Geofilters*, Warsaw, Poland, 1, 27-47.

Młynarek, J., J. Bogumił L., Andrél, R. and Gilles, B. (1991). "Soil geotextile system interaction." *Geotextiles and Geomembranes*, **10**(2), 161–176.

Palmeira, E. M. and Fannin, R. J. (2002). "Soil-geotextile compatibility in filtration." *Proceedings of the 7th International Conference on Geosynthetics*, Nice, France, Keynote Lecture, **3**, 853–869.

PIANC (1987). "Guidelines for the design and construction of flexible revetments incorporating geotextiles for inland waterways." *Supplement to Bulletin 57*, Permanent International Association of Navigation Congresses.

Rollin, A. and Lombard, G. (1988), "Mechanisms affecting long-term filtration behavior of geotextiles." *Geotextiles and Geomembranes*, **7**(1-2), 119–145.

Scheidegger, A. E. (1957), *The Physics of Flow Through Porous Media*. The MacMillan Co., NY.

Schober, W. and Teindl, H. (1979). "Filter criteria for geotextiles." *Proceedings of the 7th European Conference on Soil Mechanics and Foundation Engineering*, Brighton, UK, **2**, 121–129.